

# Adaptive Sampling for Human-aware Path Planning in Dynamic Environments

Kuanqi Cai<sup>1,2</sup>, Chaoqun Wang<sup>2</sup>, Chenming Li<sup>2</sup>, Shuang Song<sup>1</sup>, and Max Q.-H. Meng<sup>1,2</sup>

**Abstract**—Nowadays, robots are increasingly used in densely populated dynamic environments. Robots not only need to complete the navigation tasks quickly, but also need to take into account the human trajectories and the constraints of social rules. In order to avoid the robot going into the crowded areas and improve robot acceptance in the crowded public environment, we propose a human-aware motion planning algorithm that is based on sampling method. Firstly, human will be annoyed and stressed if robots disturb them during operation. To alleviate this discomfort brought by the robot, we use probabilistic representations to build the Human Domain Zone (HDZ) of individual or crowd behaviors. Besides, we propose a sampling strategy that is capable of biasing the sampling in the area where human feel comfortable or crowd is sparse. Moreover, we put forward an evaluation function to select the optimum trajectory. This function can avoid robot falling into the crowded area through VDM which is used to model the relationship between human and robot. The proposed approach is verified with extensive experiments in simulated environments. The results show that our method has the promising performance in crowded environment. It can also generate a smooth path with higher success rate.

## I. INTRODUCTION

Motion planning has gained increasing attention over the last few decades [1]. With the development of motion planning algorithms in dense environment [2], current algorithms have graceful performances in static environments and some sparsely populated environments [3]. But it remains an open problem to plan a safe and collision-free trajectory in dynamic and complex environments by taking the human comfort, crowd behavior and individual behavior into consideration.

The crowded public environments such as airport, railway station are different from structured environments. Firstly, the human trajectories in crowded public environment are affected by the baggage carried by human. Therefore, the prediction model of human trajectory in general environment is not applicable in crowded public environment. Then, in the crowded public environment, the crowds are very common in the environment. In order to avoid the robot running into the crowd, the robot should distinguish crowds and individuals. In addition, the distribution of human is uneven in the crowded public environment. Since humans are most likely to gather in some particular places like the entrance and waiting room, we should keep the robot away from these areas. Finally, to increase the human comfort, the trajectory of the

robot should cause as few conflicts as possible with human trajectory, and robot should keep an appropriate distance from human.

The collision-free and human-aware navigation is a challenging problem. To solve this problem, plenty of research has found a safe and optimal trajectory to avoid individuals or found a human comfort trajectory for Human Robot Interaction (HRI) [4]. Although some progress has been made, these methods are not suitable for complex and crowded environment. So it is important to find a systematic solution towards the target problem.

In this paper, we propose a systematic solution for motion planning in crowded and complex environment. Our method is built upon recent developments of sampling-based method while taking into consideration the human comfort and population distribution in dynamic environment. Our main contributions are listed as follows:

- First, we propose the Human Domain Zone (HDZ) to divide human into crowds and individuals which takes into consideration the baggage carried by human. After that we identify areas where pedestrians feel comfortable or uncomfortable with robots. It can also predict the next position of human in a short time.
- Second, we propose an adaptive sampling scheme which can find the safe and human-comfort areas for robot navigation in the crowded public environment.
- Third, we propose an evaluation function with Virtual Doppler Method (VDM) to find a flexible trajectory quickly in the sparsely populated areas.

Importantly, the evaluation function in each period considers the human comfort, individuals and crowds, collision probability and the distance to the target.

This paper is structured as follows. We first introduce some related work about motion planning and human-aware navigation in Section II. Then, in Section III, we give the formulation of the problem. In Section IV we explain the details of our methodology. Section V includes the experiments and results. Finally, we draw conclusions and outline the future work in Section VI.

## II. RELATED WORK

Motion planning plays an important role in the mobile robot navigation over the past few decades[5]. Plenty of research has been proposed for this topic. Some classic algorithms include Rapidly-exploring Random Tree (RRT) algorithm [6][7], Rapidly-exploring Random Tree Star (RRT\*) algorithm [8], Risk-RRT algorithm [9], and so on. These sampling-based methods can plan an optimal path to avoid

<sup>1</sup>School of Mechanical Engineering and Automation, Harbin Institute of Technology, Shenzhen, China. Email:kayle.ckq@gmail.com

<sup>2</sup>Department of Electronic Engineering, The Chinese University of Hong Kong, N.T., Hong Kong SAR, China. Email: chaoqunwang@cuhk.edu.hk, meng@cuhk.edu.hk, licmjy@link.cuhk.edu.hk

static obstacles and human. The performance of these methods is not reliable in densely populated dynamic environment.

Recently, Fiorini [10] put forward the theory of Velocity Obstacle (VO). The VO method defines a geometric region. The robot running with this velocity in this region will cause collision. There are some methods that based on VO, such as Reciprocal Velocity Obstacle (RVO) [11], Collision Avoidance under Bounded Localization Uncertainty (COCALU) [12], and Extended Velocity Obstacle (EVO) [13], were proposed to solve different problems by changing the region. These methods can be used to avoid dynamic agents which include human and other robots in the crowded environment. They assume that agents and robot have the same obstacle avoidance strategy, so these methods are not suitable for human who carries baggage in crowded public environment and it cannot prevent the robot from going into the densely area.

After that, learning-based motion planning has been widely used in recent years. Chen *et al.* [14] proposed a decentralized multi-agents collision avoidance algorithm based on deep reinforcement learning, which can accurately predict the trajectory of human. Some researchers proposed a method named SA-CALDRL [15] which can solve the randomness of human behaviors in the robot navigation. Everett [16] extended the SA-CALDRL algorithm to GA3C-CADRL method by introducing the LSTM method [17] in the algorithm. GA3C-CADRL does not require any knowledge of human dynamics. The above methods can predict more accurate trajectory of human, and use these trajectories as a reference factor for robot motion planning to prevent the robot from entering crowded region. Yet above methods cannot distinguish crowds and individuals, and it cannot consider the human comfort.

Besides, several methods have been supposed for human-aware navigation. Manuel *et al.* [18] proposed a path planning method which took into account the safety of human in warehouses. Vaibhav *et al.* [19] combined the local planner and human motion prediction to make an optimal path in the factory test environment. Marina *et al.* [20] used human path and social cost function to plan a human-aware trajectory. The above algorithms show good results on individuals, but they cannot perform well for the crowds.

We propose a sampling-based path planning scheme that uses an advanced adaptive sampling strategy to reduce the risk of collision and increase the human comfort in the dynamic environment. Then, we propose the VDM to find sparsely populated areas. We also design the trajectory optimal evaluation function to select an optimum and soft path.

### III. PROBLEM FORMULATION

The major objective for motion planning in densely populated dynamic environment is to finish the navigation task in a timely manner while simultaneously avoid the robot falling into the crowd and reduce the discomfort of human. The map is represented by  $\mathcal{M} \in \mathbb{R}^n$ .  $\mathcal{H}(t)$  is the possible collision

field. The map is updated in real time as  $\mathcal{M}(t)^*$  in time  $t$ .  $\mathcal{X}(t)$  be the state of the inanimate obstacles in the map,

$$\mathcal{M}(t)^* = \mathcal{M} - \mathcal{H}(t) - \mathcal{X}(t), \quad (1)$$

where  $x_r(t)$  be the state of the robot at the time  $t$ , and  $u(t)$  be the control input of robot. The robot dynamic function  $f$  can be depicted as:

$$x_r(t) = f(x_r(t-1), \mathbf{u}(t-1), \eta_n), \quad \eta_n \sim \mathcal{N}(\mathbf{0}, M_t), \quad (2)$$

The  $\eta_t$  represents the motion noise following the Gaussian distribution with zero mean and the variance of  $M_t$ . Our motion planning method is to find an optimal trajectory  $\mathbf{L}(\mathbf{x}) = \{x_1, \dots, x_T\}$  with the initial point is  $x_1 = x_{init}$  and the terminal state is  $x_T$ . All the states are in the free space and they are constrained by the human awareness.

Let  $\mathbb{Z}$  be a set of trajectories. The optimal motion planning is defined as searching for the best trajectory  $\mathbf{L}^*(\mathbf{x})$  that minimizes the given cost function  $\bar{\delta}$ .

$$\begin{aligned} \mathbf{L}^*(\mathbf{x}) &= \arg \min_{\mathbf{L}(\mathbf{x}) \in \mathbb{Z}} \bar{\delta}(\mathbf{L}(\mathbf{x})) \\ \text{s.t. } & \mathbf{L}(x_1) = x_{init} \\ & \mathbf{L}(x_T) \in \{d(x_T, x_{goal}) < r\} \\ & \mathbf{L}(x_t) \in \mathcal{M}(t)^*, \forall t \in [0, T] \\ & \mathcal{Q} < \partial \rightarrow x_t \in \mathcal{M}'(t), \end{aligned} \quad (3)$$

The  $\mathcal{M}'(t)$  is a map considering the human comfort. The  $\mathcal{Q}$  is occupancy rate which is used to describe the density of pedestrians in the robot working area. The  $\partial$  is a threshold for crowd density. As indicated in Eq. 3, the main aim of this method is to plan a feasible path that avoids both static and dynamic objects while considering the unique social attributes of human in crowded public environment.

### IV. METHODOLOGY

In this paper, our method is based on Risk-RRT\* algorithm[21]. The proposed motion planning algorithm can generate an optimal and feasible path in the crowded public environment. Our method is divided into three parts. 1) The information about the human is obtained by the robot with sensors continuously. Then, a method using HDZ based information is proposed to analyze the relationship between individuals or crowds in environment. This relationship is described by the probabilistic representations and is included in the  $\mathcal{M}(t)$ . 2) We propose the adaptive sampling method **Sample**( $\cdot$ ) to generate a series of sampling points  $\mathcal{SP} = \{sp_1, sp_2, \dots, sp_m\}$  where  $\mathcal{SP} \in \mathcal{M}(t)^*$  or  $\mathcal{M}'(t)$  by analysing the density of human. Only one sampling point can be selected as the direction of the next state for the robot. 3) We propose an evaluation function  $\bar{\delta}$  including VDM. The probability of collision, the risk of falling into the crowd and the cost from the generated trajectory to the goal target will be evaluated by the  $\bar{\delta}$ . Through this function, we can get the best path in  $\mathcal{M}(t)^*$ . In order to get the best trajectory in the dynamic environment, motion planning and chassis control will be carried out simultaneously in each period.

In the following parts, we will detail how to generate the optimum trajectory in each period.

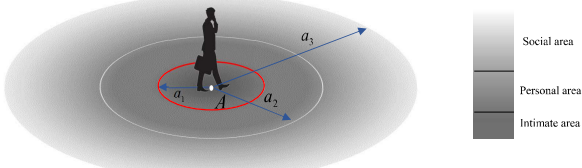


Fig. 1: Personal field. The coordinates of the human is  $A : (x_1, y_1)$ .  $a_1$  is the intimate distance.  $a_2$  is the personal distance.  $a_3$  is the social distance. The color from deep to shallow represents the different impact of areas on human. The darker the area, the greater impact on human. The white circles represent the dividing line between different areas in personal field.

#### A. Human Domain Zone

It is important to make human feel safe and comfortable in the crowded public environment. So, in this section, we build individual and crowd models from psychological perspective. These models serve as prior knowledge of robot navigation.

Psychologists such as Hall *et al.* [22] divided the distance between people in a dynamic environment into four categories. They are intimate distance, personal distance, social distance and public distance. Motivated by this, we define the personal field in the map. The personal field is a concentric circular with human coordinates as the circle center and the different distance as the radius. As we can see in the Fig. 1. The personal field consists of intimate area, personal area and social area. In order to avoid collision with pedestrians, the robot should avoid entering the intimate area during the motion planning. The personal area is ideal area for human-robot interaction.

In the crowded public environment, most human carry baggage or baggage car. When the robot is too close to the baggage or human, the baggage owner might feel uncomfortable and the potential collision risk will increase. Besides, in these environments people who know each other often travel in crowds. Human-aware navigation needs robot to consider the relationship between human in the crowd. Therefore, the personal field will be not only expanded by the number and the volume of the baggage but it also expended by the interpersonal relationship. The process of building the model can be divided into two steps:

Firstly, We divide people into individuals and crowds in the environment. If the distance between people is less than the personal distance, they are believed to form a group. Individuals in the environment are grouped with their baggage. The baggage car and human in the group are all approximated as some points.

Secondly, we use a smallest circle  $C_i$  that wraps these points. Center  $X_{hc}(t)(x_c, y_c)$  and radius  $r_c$  of  $C_i$  are recorded. The formula of the crowd model is defined as follows. The parameter  $\Upsilon$  represents the baggage area cost, which is half of the average length of all baggage. Fig. 2



Fig. 2: Expended personal field. The red points are leftmost point ( $P_l$ ), rightmost point ( $P_r$ ), top point ( $P_t$ ), bottom point ( $P_b$ ), the blue points are the inner points, and the white circle is the dividing line between the personal field and the social field. The red circle is the smallest circumscribed circle of the point set, and it also the intimate area in expended personal field. The radius of this circle is expended intimacy distance.

shows the expended personal field of series people.

$$\begin{cases} (x - x_c)^2 + (y - y_c)^2 = (d + r_c + \Upsilon)^2 \\ d \in \{d_{\text{personal}}, d_{\text{social}}, d_{\text{public}}\}, \end{cases} \quad (4)$$

In a dynamic environment, the position of individuals and crowds vary with time. So, in each time period, we should not only calculate the current personal field or crowd field, but we also predict the future. For crowd motion, we assume that the size of the expended personal field is constant and the position of the crowd in the map is changing. In this paper, the time period  $[t^*, t^* + \Delta t]$  is short enough that we can use the velocity of the individuals or crowds observed at time  $t^*$  to approximate the velocity within the period. Without loss of generality, we assume that the velocity of the crowd is the average velocity of all human in the crowd. After that we can calculate the personal field and expended personal field at time  $t^* + \Delta t$ . We use HDZ to represent these fields during  $\Delta t$ . As shown in Fig. 3 the red region which we define as possible collision field  $\mathcal{H}$  is the intimate area during  $\Delta t$  in HDZ. The white region named interaction area  $\mathcal{V}(t)$  is the sum of the personal areas, and the grey region named planning area  $\mathcal{W}(t)$  is the sum of social areas.

#### B. Adaptive sampling

The sample function  $\text{Sample}(\cdot)$  we proposed is different from the random sampling method in the map. Our method can sample the points in the area that we are interested in. So we can most likely get an optimum point to guide the robot.

Before executing the navigation task, the robot obtains the original map through sensors. The origin map  $\mathcal{M}(t)$  at time  $t$  contain two regions, they are feasible region and occupied region. The occupied region is composed by the possible collision field  $\mathcal{H}$  and inanimate obstacles  $\mathcal{X}(t)$  at time  $t$ . Before scattering points, we should update map  $\mathcal{M}(t)$  to  $\mathcal{M}^*(t)$  with obstacles, human, etc in Eq. 1.  $\mathcal{M}^*(t)$  only contains viable region. In process of human-aware

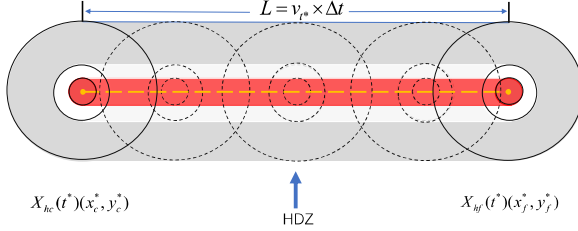


Fig. 3: Human Domain Zone (HDZ).  $v_{t*}$  is the velocity of the individual or crowd at time  $t^*$ . The dotted black lines indicate the different positions of human during  $\Delta t$  at different times. The yellow line is the track of human movement.  $L$  is the length of human trajectory during  $\Delta t$ . The position at time  $t^*$  is  $X_{hc}(t^*)(x_c^*, y_c^*)$ , and the position at time  $t^* + \Delta t$  is  $X_{hf}(t^*)(x_f^*, y_f^*)$ .

navigation, the robot should consider the human awareness. The formula for  $\mathcal{M}'(t)$  is shown below.

$$\mathcal{M}'(t) = \mathcal{M} - \mathcal{H}(t) - \mathcal{X}(t) - \mathcal{V}(t), \quad (5)$$

However, in some densely populated areas, excessive consideration of human comfort will cause the sampling area  $\mathcal{M}'(t)$  so small that the “freezing robot” problem [23] will happen. To solve this problem, we propose to count the number of human in the robot working area. It is important to design the robot working area in proper size. If size is too small, we will ignore the potential human which will cause the congestion in the next time period. The working area of the robot is divided into two parts in this paper, the first part is Maximum Probability Work Area (*MPWA*). The diameter of *MPWA* is the distance from the initial point of robot to the target point. The second part is Possible Working Area (*PWA*). The radius of *PWA* is equal to the radius of *MPWA* plus a public distance. The formula for  $\mathcal{Q}$  in Eq. 3 is shown below.

$$\mathcal{Q} = \sum_{i=1}^{N_1} P_{MPWA} + \sum_{i=1}^{N_2} P_{PWA}, \quad (6)$$

In this formula,  $N_1$  and  $N_2$  refer to the number of human in the *MPWA* and *PWA* areas.  $P_{MPWA}$  and  $P_{PWA}$  refer to the probabilities that humans will appear.  $P_{MPWA}$  ranges from  $\Omega_i$  to  $\Omega_j$  according to the distance between human and the center of the robot working area.  $P_{PWA}$  ranges from  $\Omega_o$  to  $\Omega_p$ .

As the environment changes over time, sampling and map updates are executed each period. The smaller the time period, the more accurate the perception of the dynamic environment will be.

### C. Evaluation function of trajectory

The evaluation function is related to the collision risk  $\mathcal{C}_\nabla$ , the cost of distance  $C_d$ , and the cost of human effects  $\mathcal{A}$  generated by VDM. The formula is denoted as:

$$\bar{\delta} = w_1 \mathcal{C}_\nabla + w_2 C_d + w_3 \mathcal{A}, \quad (7)$$

where  $w_1, w_2, w_3$  are the weights for balancing the quantities. Three parameters need to be normalized. We aim to minimize  $\bar{\delta}$  in each time period. The definition of collision risk  $\mathcal{C}_\nabla$  and cost of distance  $C_d$  are the same as Risk-RRT\* method. The weights  $w_1, w_2, w_3$  are designed according to the environments. The weight of  $\mathcal{A}$  is based on Doppler Effect [24]. According to Doppler Effect, the robot is regarded as the sound source. We assume that robot radiates a virtual wave, and each human is equal to an observer. We also divide the relation between human and robot into four parts. a) Humans get close to the robot. b) Humans are far from the robot. c) Robot remains relatively stationary with people. d) The robot is far away from humans. Then, we use the virtual receiving frequency  $f'$  to express the effects from the robot to the human. Because the effects are mutual,  $f'$  also express the effects from human to robot.  $f'$  is similar to the frequency in the Doppler Effect. The different relationships between human and robots cause the different values of virtual receiving frequency  $f'$ . When the robot gets close to the human from different angles, the distance between human and robot will decrease. The virtual receiving frequency received by the human increases continuously. We can see the Human1 in Fig. 4. When the distance between the robot and the human increase, for example the robot and human move in the opposite direction, the virtual receiving frequency of the human receiving from robot will decrease. We can see the Human3 in Fig. 4. For the Human2, the distance between the robot and human is so far that we assume the  $f'$  received by the human being is zero. That is, when the human is outside the scope of the robot working area, human and robot do not affect each other. If the human and the robot maintain the constant distance, the human will receive a constant non-zero virtual receiving frequency, as shown by Human4 in the figure.

We can calculate the value of  $f'$  corresponding to each person in the robot working area when the robot is at any position of the trajectory. We accumulate the  $f'$  that everyone receives as the influence frequency  $f^*$  of the robot at that position. The smaller the influence frequency  $f^*$ , the fewer human around the robot. So we can use it to select the optimum trajectory of the robot to avoid crowd.

The value of the virtual receiving frequency  $f'$  received by human is related to the virtual frequency  $f$  of the virtual wave that is sent by the robot. We assume that the wavelength is  $\lambda$ , the value of the virtual wavelength is social distance, and the virtual frequency  $f$  can be represented by the virtual wavelength and the virtual speed  $v$  of the robot. The virtual speed is related to the medium. The medium  $n$  defined in this paper is positively related to the human occupation ratio in operation region. That is, the robot works in a large medium environment with higher human occupation ratio. So the robot's virtual speed is slow. The virtual speed of the robot will be quicker when the robot works in a small medium environment with lower human occupation ratio. The origin point is  $O(x_o, y_o)$  and the target point is  $T(x_t, y_t)$ . The

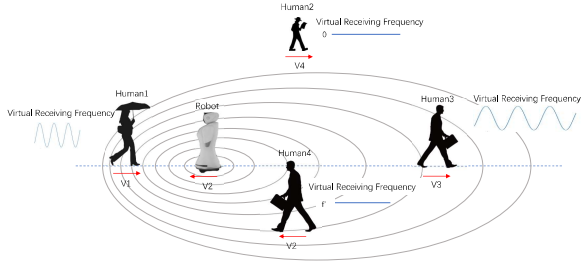


Fig. 4: Virtual Doppler Method. The blue line in the figure indicates the virtual receiving frequency, and the red arrow indicates the direction of movement of the human or the robot. The circles on the ground are the virtual wave generated by the robot. The virtual wave is what we assume is not real.

equation of medium  $n$  is:

$$n = \frac{\delta}{s}, \quad (8)$$

In this equation,  $s$  is the robot working area,  $\delta$  is the sum area of human and baggage at the initial moment. So we can get the equation of virtual frequency  $f$  as:

$$f = \frac{v * \cos(\arctan \frac{y_t - y_o}{x_t - x_o})}{\lambda} * n, \quad (9)$$

The virtual receiving frequency received by the receiver can also be divided into three models.

First, when the human is stationary in the environment and the robot is in motion, the virtual receiving frequency received by the person is:

$$f' = \frac{v}{v \pm (\lambda_1 * v_{robot\_pre} + \lambda_2 * v_{robot\_cur}) * \cos \alpha'} * f, \quad (10)$$

the  $\alpha'$  is the angle between the speed direction of the robot and the direction of the robot to the human.  $v_{robot\_pre}$  is the velocity of the robot at last moment and  $v_{robot\_cur}$  is the velocity of robot at the current moment.  $\lambda_1$  is the weight of  $v_{robot\_pre}$ , and  $\lambda_2$  is the weight of  $v_{robot\_cur}$ .

Second, when the robot is stationary and the human is moving in the environment, the virtual receiving frequency is:

$$f' = \frac{v \pm (\lambda_1 * v_{human\_pre} + \lambda_2 * v_{human\_cur}) * \cos \beta'}{v} * f, \quad (11)$$

the  $\beta'$  is the angle between the speed direction of the human and the direction of the human to the robot.  $v_{human\_pre}$  is the velocity of the robot at last moment and  $v_{human\_cur}$  is the velocity of robot at the current moment.

Third, in most of the time, human and robots are moving in dynamic environment with different trajectories. The robot may get close to human or away from human. The virtual receiving frequency is:

$$f' = \frac{v \pm (\lambda_1 * v_{robot\_pre} + \lambda_2 * v_{robot\_cur}) * \cos \beta'}{v \pm (\lambda_1 * v_{human\_pre} + \lambda_2 * v_{human\_cur}) * \cos \alpha'} * f, \quad (12)$$

Among the above three models, when the robot is approaching the human being, the '+' sign will be taken. When the robot is getting away from human, the '-' sign will be taken.

## V. EXPERIMENTS AND RESULTS

To verify the effectiveness of the proposed algorithm, we carry out experiments in some simulation environments. For the software, we use Risk-RRT package in Robot Operating System(ROS) of Kinetic version released on Ubuntu16.04 LTS. The simulation environments are built in *Ros stage* simulator. The robot in simulator is equipped with RGB-D camera and hukuyo lidar. In this paper, the path planning algorithm in Risk-RRT package is replaced by ours and Risk-RRT\*. In order to simulate the crowded public environment more realistically, we not only set individuals but also crowds in the environment. We used Monte Carlo stochastic simulation to generate the amount of baggage, the area of baggage and the amount of human in the crowd. In order to show the discomfort to human caused by robot, we use circles with different colors and sizes to represent the personal areas of the individuals or crowds. We set the *Discomfort Number* (DN) to calculate the times of robot entering the personal area. This parameter is used to evaluate whether the path of the robot will cause discomfort to human. The radius of the personal area is calculate by the model above. We also use the solid circles to represent the positions of individuals or crowds at the current moment, and the dotted circles represent the initial positions of them. For crowds in the environment, we ignore the individual behavior in the crowd and we use the trajectory of the the personal field center to approximate the trajectory of the crowd.

### A. Weight verification

When selecting the best trajectory, the robot should stay as far away from pedestrians as possible and reach the destination as quickly as possible. So in the the equation 7, it is important for us to select the correct value of  $w3/w2$ . If the influence of  $C_d$  on the trajectory is greater than  $\mathcal{A}$ , the robot will plan a longer trajectory. If the influence of  $C_d$  is too large, robot will move into crowded areas in order to reach the destination as soon as possible.

In this paper, the value of  $\alpha = w3/w2$  obtained by the entropy weight method is 0.128. In order to verify that the  $\alpha$  obtained by the entropy weight method is optimum solution, we make comparative experiments. The five values of  $\alpha$  we selected are 0.1, 0.128, 0.2, 0.5 and 0.8. These values of  $\alpha$  are so close that they have the similar effects on human avoidance. So we use the parameters of time and path length as evaluation indexes to find the optimal value. The experimental results are shown in Fig. 5. As we can see from the simulation environments, three independent humans ( $H_1(t)$ ,  $H_2(t)$  and  $H_3(t)$ ) start at the same time, but the speeds and directions are different. The initial position of the robot is (3, 3), the target position is (25.5, 24). The three subgraphs correspond to the trajectories of five different weights when  $t1=25.5$ s,  $t2=51$ s, and  $t3=76.8$ s. We performed

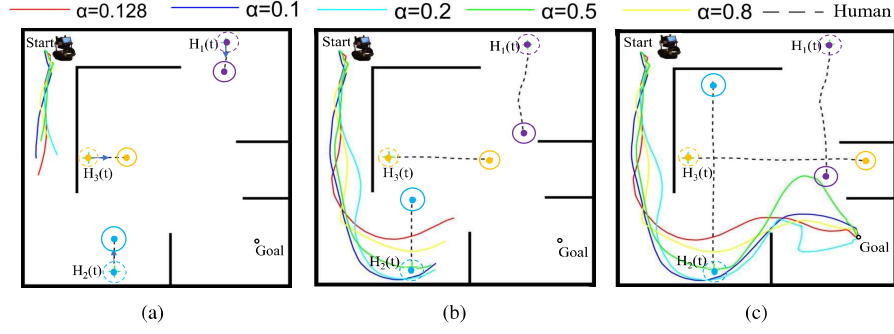


Fig. 5: The experiment of weight. The black dotted lines are the trajectory of the humans. The blue arrows represent their directions of movement. The trajectories generated by the  $\alpha = 0.128$ ,  $\alpha = 0.1$ ,  $\alpha = 0.2$ ,  $\alpha = 0.5$  and  $\alpha = 0.8$  are shown in red, navy blue, light blue, yellow and green lines, respectively.

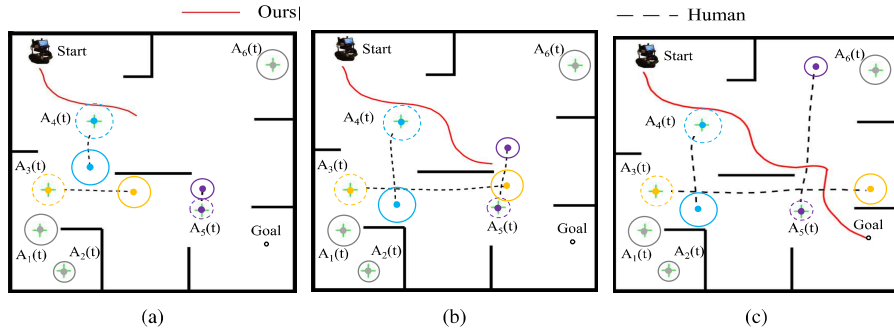


Fig. 6: Feasibility experiment. The initial position of the robot is (3.6, 3.6), the target position is (26.4, 23.1). Three subgraphs correspond to the trajectories of five different weights when  $t_1=30$ s,  $t_2=63$ s, and  $t_3=75.3$ s.

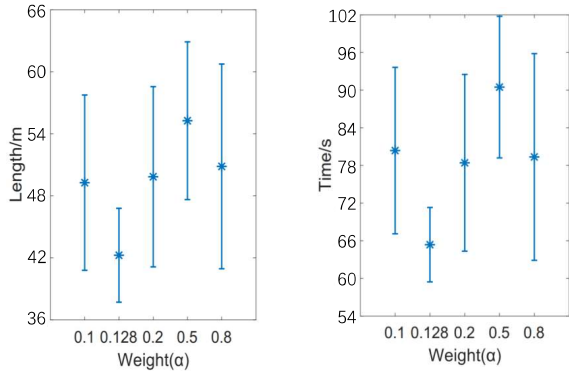


Fig. 7: Error bar graph of weights experiment. The length of the error bar graph is the twice of the variance, and the point in the error bar is the average.

ten repeated experiments on each  $\alpha$ . Then we draw error bar graphs in Fig. 7.

As we can see from the Fig. 7, the experiment with  $\alpha = 0.128$  finds the shortest path in the shortest time. The variance is the smallest among all  $\alpha$ . Therefore, it can be seen from experiments that the  $\alpha = 0.128$  calculated by the entropy weight method has the best performance.

### B. Feasibility experiment in dense environment

To verify the feasibility of the algorithm in densely populated environments, we simulated a crowded public environment. As we can see in the Fig. 6.

In this environment, We set up three crowds and four individuals. Two crowds( $A_4(t)$ ,  $A_6(t)$ ) and three individuals( $A_3(t)$ ,  $A_7(t)$ ,  $A_8(t)$ ) are in motion. One crowd( $A_1(t)$ ) and two individuals are at rest. The experiment is repeated ten times in the same environment. We record the experimental data in Table I.

From the experimental results, our algorithm can make the robot avoid the dense crowd in the environment to reach the target point. And the trajectory of our method can avoid all personal areas, that is, human do not feel repulsive to the robot in our method. The above experiment shows that our algorithm has a good performance in the crowded public environment.

### C. Comparative experiments

We compared with Risk-RRT\*, which is an advanced risk-based motion planning algorithm to verify the feasibility of our algorithm. We test our method in two simulated environments with different numbers of humans. Fig. 8 shows the result of comparison simulation environments.

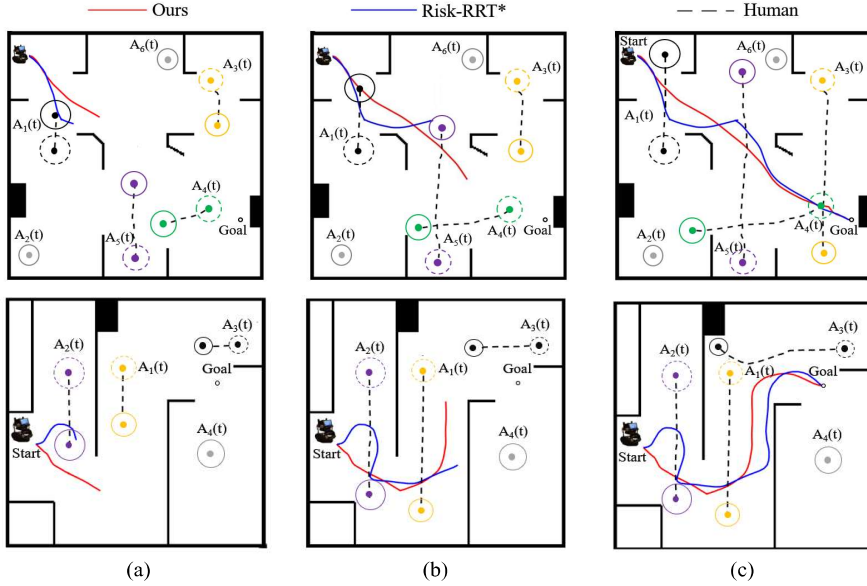


Fig. 8: Comparative experiments. The blue trajectory is under Risk-RRT\* method, and red trajectory is under our method. In the first environment, one crowd ( $A_1(t)$ ) and three individuals ( $A_3(t)$ ,  $A_4(t)$ ,  $A_5(t)$ ) are dynamic. Two individuals ( $A_2(t)$ ,  $A_6(t)$ ) are static. The initial position of the robot is (3, 3), and the end position is (27, 22.5). The three subgraphs of first environment correspond to different time,  $t_1=27s$ ,  $t_2=45s$ , and  $t_3=85s$ , respectively. In the first row, one crowd ( $A_2(t)$ ) and two individuals ( $A_1(t)$ ,  $A_3(t)$ ) are dynamic. One crowd  $A_4(t)$  is static. The initial position of the robot is (3.9, 17.4), the end position is (24, 10.5). The three subgraphs of the second environment correspond to different time,  $t_1=27s$ ,  $t_2=48s$ , and  $t_3=90s$ , respectively.

TABLE I: Feasibility Experimental Data of Simulation Environment

Parameters	Group		Mean/s	Time Max/s	Min/s	Mean/m	Length Max/s	Min/s	DN
	Static	Dynamic							
Test Scenario	4	3	75.3	83.4	66.9	36.21	41.4	34.8	2

TABLE II: Feasibility Experimental Data of Simulation Environment

Parameters		Time/s	Length/m	DN
First Environment	Ours	72.5	34.38	18
	Risk-RRT*	84.48	37.26	2
Second Environment	Ours	76.11	40.5	9
	Risk-RRT*	89.76	45.48	1

The first row in Fig. 8 is the first simulation environment, and the second row is second simulation environment. As we can see from the two experiments, the trajectory planned by our algorithm is smoother. Because the red trajectory has taken into account the positions of the pedestrians at the next moment, the robot reduces the number of changing trajectory. The change of the trajectory is to avoid collision between human and robot. In addition, simulation experiments have proved that our algorithm uses less time and shorter trajectory to reach the destination than the Risk-RRT\* algorithm. The experimental data is shown in Table II.

For human comfort, the trajectory planed by our method can reduce the times that the robot enter the personal area. In the first experimental environment, the trajectory under the Risk-RRT\* will make the robot entering the personal area

of  $A_1(t)$  and  $A_5(t)$ . In the second environment, the robot will enter the personal area of  $A_2(t)$ . This is not good for human-robot interact in the comfortable environment and it will greatly increase the potential collision.

In a word, our method can guarantee the comfort of human in the environment, and plan a smooth and short trajectory.

## VI. CONCLUSIONS AND FUTURE WORK

In this paper, we put forward a sampling-based path planning algorithm that aims to planning a human-aware and smooth path to avoid robot falling into dense area. A number of experiments we carried out prove the effectiveness of our algorithm. The purpose of dynamic sampling is to spread the sample points to a sparsely populated area. By comprehensively considering the human comfort, human relationship and the position of the human at next moment, the proposed algorithm can quickly find a smooth and short trajectory while reducing the collision probability. The proposed method is verified in feasibility experiment and comparative experiments. These experiments prove the advantages of the proposed algorithm.

In the future, we will further investigate the interpersonal relationship in the crowd under the crowded public environment. Then, we will propose a more accurate trajectory

prediction model of the crowd for robot motion planning to reduce the possibility of collision.

## REFERENCES

- [1] Chaoqun Wang, Wenzheng Chi, Yuxiang Sun, and Max Q-H Meng. Autonomous robotic exploration by incremental road map construction. *IEEE Transactions on Automation Science and Engineering*, 2019.
- [2] Delong Zhu, Tingguang Li, Danny Ho, and Max Q-H Meng. Deep reinforcement learning supervised autonomous exploration in office environments. In *Robotics and Automation (ICRA), 2018 IEEE International Conference on*. IEEE, 2018.
- [3] Chaoqun Wang, Jiyu Cheng, Jiankun Wang, Xintong Li, and Max Q-H Meng. Efficient object search with belief road map using mobile robot. *IEEE Robotics and Automation Letters*, 3(4):3081–3088, 2018.
- [4] Thibault Kruse, Amit Kumar Pandey, Rachid Alami, and Alexandra Kirsch. Human-aware robot navigation: A survey. *Robotics and Autonomous Systems*, 61(12):1726–1743, 2013.
- [5] Chaoqun Wang, Delong Zhu, Teng Li, Max Q-H Meng, and Clarence W de Silva. Efficient autonomous robotic exploration with semantic road map in indoor environments. *IEEE Robotics and Automation Letters*, 4(3):2989–2996, 2019.
- [6] Steven M LaValle. Rapidly-exploring random trees: A new tool for path planning. 1998.
- [7] Chaoqun Wang and Max Q-H Meng. Variant step size rrt: An efficient path planner for uav in complex environments. In *2016 IEEE International Conference on Real-time Computing and Robotics (RCAR)*, pages 555–560. IEEE, 2016.
- [8] Fahad Islam, Jauwairia Nasir, Usman Malik, Yasar Ayaz, and Osman Hasan. Rrt-smart: Rapid convergence implementation of rrt towards optimal solution. In *2012 IEEE International Conference on Mechatronics and Automation*, pages 1651–1656. IEEE, 2012.
- [9] Chiara Fulgenzi, Anne Spalanzani, Christian Laugier, and Christopher Tay. Risk based motion planning and navigation in uncertain dynamic environment. 2010.
- [10] Paolo Fiorini and Zvi Shiller. Motion planning in dynamic environments using velocity obstacles. *The International Journal of Robotics Research*, 17(7):760–772, 1998.
- [11] Jamie Snape, Jur Van Den Berg, Stephen J Guy, and Dinesh Manocha. Independent navigation of multiple mobile robots with hybrid reciprocal velocity obstacles. In *2009 IEEE/RSJ International Conference on Intelligent Robots and Systems*, pages 5917–5922. IEEE, 2009.
- [12] Daan Bloembergen, Karl Tuyls, Daniel Hennes, and Michael Kaisers. Evolutionary dynamics of multi-agent learning: A survey. *Journal of Artificial Intelligence Research*, 53:659–697, 2015.
- [13] Amichai Levy, Chris Keitel, Sam Engel, and James McLurkin. The extended velocity obstacle and applying orca in the real world. In *2015 IEEE International Conference on Robotics and Automation (ICRA)*, pages 16–22. IEEE, 2015.
- [14] Yu Fan Chen, Miao Liu, Michael Everett, and Jonathan P How. Decentralized non-communicating multiagent collision avoidance with deep reinforcement learning. In *2017 IEEE international conference on robotics and automation (ICRA)*, pages 285–292. IEEE, 2017.
- [15] Yu Fan Chen, Michael Everett, Miao Liu, and Jonathan P How. Socially aware motion planning with deep reinforcement learning. In *2017 IEEE/RSJ International Conference on Intelligent Robots and Systems (IROS)*, pages 1343–1350. IEEE, 2017.
- [16] Michael Everett, Yu Fan Chen, and Jonathan P How. Motion planning among dynamic, decision-making agents with deep reinforcement learning. In *2018 IEEE/RSJ International Conference on Intelligent Robots and Systems (IROS)*, pages 3052–3059. IEEE, 2018.
- [17] Felix A Gers, Jürgen Schmidhuber, and Fred Cummins. Learning to forget: Continual prediction with lstm. 1999.
- [18] Manuel Fernandez Carmona, Tejas Parekh, and Marc Hanheide. Making the case for human-aware navigation in warehouses. In *Annual Conference Towards Autonomous Robotic Systems*, pages 449–453. Springer, 2019.
- [19] Vaibhav V Unhelkar, Przemyslaw A Lasota, Quirin Tyroller, Rares-Darius Buhai, Laurie Marceau, Barbara Deml, and Julie A Shah. Human-aware robotic assistant for collaborative assembly: Integrating human motion prediction with planning in time. *IEEE Robotics and Automation Letters*, 3(3):2394–2401, 2018.
- [20] Marina Kollmitz, Kaijen Hsiao, Johannes Gaa, and Wolfram Burgard. Time dependent planning on a layered social cost map for human-aware robot navigation. In *2015 European Conference on Mobile Robots (ECMR)*, pages 1–6. IEEE, 2015.
- [21] Wenzheng Chi and Max Q-H Meng. Risk-rrt: A robot motion planning algorithm for the human robot coexisting environment. In *2017 18th International Conference on Advanced Robotics (ICAR)*, pages 583–588. IEEE, 2017.
- [22] Edward T Hall, Ray L Birdwhistell, Bernhard Bock, Paul Bohannan, A Richard Diebold Jr, Marshall Durbin, Munro S Edmonson, JL Fischer, Dell Hymes, Solon T Kimball, et al. Proxemics [and comments and replies]. *Current anthropology*, 9(2/3):83–108, 1968.
- [23] Peter Trautman and Andreas Krause. Unfreezing the robot: Navigation in dense, interacting crowds. In *2010 IEEE/RSJ International Conference on Intelligent Robots and Systems*, pages 797–803. IEEE, 2010.
- [24] Sidhant Gupta, Daniel Morris, Shwetak Patel, and Desney Tan. Soundwave: using the doppler effect to sense gestures. In *Proceedings of the SIGCHI Conference on Human Factors in Computing Systems*, pages 1911–1914. ACM, 2012.